Astronomy & Astrophysics manuscript no. ms˙v8
January 10, 2012

The Effects of Orbital Environment on X-ray CCD Performance

Catherine E. Grant, Beverly LaMarr, Eric D. Miller, and Marshall W. Bautz

Kavli Institute for Astrophysics and Space Research, Massachusetts Institute of Technology, Cambridge, MA 02139, USA e-mail: cgrant@space.mit.edu

ABSTRACT

Context. The performance of CCD detectors aboard orbiting X-ray observatories slowly degrades due to accumulating radiation damage.
Aims. In an effort to understand the relationship between CCD spectral resolution, radiation damage, and the on-orbit particle background, we attempt to identify differences arising in the performance of two CCD-based instruments: the Advanced CCD Imaging Spectrometer (ACIS) aboard the Chandra X-ray Observatory, and the X-ray Imaging Spectrometer (XIS) aboard the Suzaku X-ray Observatory.
Methods. We compare the performance evolution of front- and back-illuminated CCDs with one another and with that of very similar detectors installed in the ACIS instrument aboard *Chandra*, which is in a much higher orbit than *Suzaku*. We identify effects of the differing radiation environments as well as those arising from structural differences between the two types of detector.
Results. There are some differences and these are they.

Key words. some keywords

1. Introduction

Charged-coupled devices (CCDs) as astronomical X-ray detectors have become nearly ubiquitous since their their first use in sounding rocket flights in the late 1980s. CCDs provide excellent quantum efficiency with moderate spectral resolution over a broad energy range (∼0.1–10 keV) and are well-suited as imaging spectrometers as well as readout detectors for dispersive gratings. Currently, CCDs are focal plane detectors in five operating spacecraft from NASA, ESA and JAXA, and are planned to be part of many upcoming missions.

Radiation damage is a common concern in all spacecraft components. One symptom of radiation damage in CCDs is an increase in the number of charge traps. When charge is transfered across the CCD to the readout, some portion can be captured by the traps and gradually re-emitted. If the original charge packet has been transfered away before the traps re-emit, the captured charge is "lost" to the charge packet. The pulseheight read out from the instrument which corresponds to a given energy decreases with increasing transfer distance. This process is quantified as charge transfer inefficiency (CTI), the fractional charge loss per pixel. In addition, the spectral resolution increases due to noise in the charge trapping and re-emission process, non-uniform trap distribution, and variations in trap occupancy (further discussed in the next paragraph). All of these processes apply to the charge in each pixel, so multi-pixel events will be more degraded than single-pixel events.

Measured CTI is a function of fluence, or, more specifically, the amount of charge deposited on the CCD. As the fluence increases, traps filled by one charge packet may remain filled as a second charge packet is transferred throught the pixel. The second charge packet sees fewer unoccupied traps as a result of the previous "sacrificial charge" and loses less charge than it would have otherwise (Gendreau et al. 1993). This sacrificial charge can be in the form of X-rays, charged particle interactions, or intentionally injected charge.

The response of a CCD-based instrument is thus partially determined by its particle environment, whether causing radiation damage or providing sacrificial charge, which in turn is dependent on the spacecraft orbit. The Advanced CCD Imaging Spectrometer (ACIS) on the *Chandra X-ray Observatory* and the X-ray Imaging Spectrometer (XIS) on *Suzaku* utilize similar CCDs but occupy very different radiation environments. The two instruments combined have produced more than eighteen years worth of monitoring data which provides a unique opportunity to better understand the relationship between CCD spectral resolution, radiation damage, and the on-orbit particle background.

We begin by describing the differences and similarities of the instruments, spacecraft orbits, and on-board calibration sources in Section 2. Section 3 outlines our data analysis procedures while Section 4 discusses the results.

2. Description of the Instruments

2.1. CCD Detector Characteristics

The CCD chips in ACIS and the XIS were fabricated at MIT Lincoln Laboratory and are very similar in design. The ACIS CCDs predate the XIS CCDs by nearly a decade so some small differences do exist.

Chandra has a single X-ray telescope and a moveable Science Instrument Module (SIM), which can move ACIS in and out of the telescope focus. The ACIS focal plane consists of ten CCD devices (model CCID17), eight of which are front-illuminated (FI) and two of which are back-illuminated (BI). The layout of the ACIS devices is shown in Figure 1. The CCD characteristics are summarized in Table 1 and described in detail by Garmire et al. (2003).

Suzaku has four XIS instruments, each with an independent X-ray Telescope (XRT) and focal plane assembly. The four devices are model CCID41, comprising three FI chips (XIS0, XIS2, and XIS3) and one BI (XIS1). The layout of the XIS de-

vices is shown in Figure 2. One of the FI devices (XIS2) was damaged by a likely micrometorite strike in October 2006 and has been unused since that time. The CCDs are summarized in Table 1 and described in detail by Koyama et al. (2007). The XIS devices are physically very similar to the ACIS devices with one notable exception, the addition of charge injection capabilities in the XIS CCID41 (Bautz et al. 2007).

While the CCDs are reasonably similar, there are a number of important operational differences. The individual frame exposure time for XIS is more than twice as long as for ACIS. Given the same particle or X-ray flux, the longer frame time of XIS will yield more sacrificial charge than seen on ACIS. Another important difference is the operating temperature of the detector. ACIS is kept much colder than XIS, which reduces incidence of warm pixels. Depending on the characteristics of the electron traps, the temperature can also change the measured CTI. In the case of the ACIS BI CCDs, the initial CTI is all due to damage during manufacturing, and the performance is slightly better at warmer temperatures. The CTI of the ACIS FI CCDs is entirely due to radiation damage, so the CCDs are highly sensitive to temperaure and have much lower CTI at -120°C.

2.2. Orbital Radiation Environments

ACIS and XIS occupy quite different radiation environments. *Chandra* is in a highly elliptical, 2.7-day orbit that transits a wide range of particle environments, from the Earth's radiation belts at closest approach through the magnetosphere and magnetopause and past the bow shock into the solar wind. Soon after launch it was discovered that the FI CCDs had suffered radiation damage from exposure to soft protons (~0.1–0.5 MeV) scattered off *Chandra's* grazing-incidence optics during passages through the radiation belts. The BI CCDs were unaffected due to the much deeper buried channel. Since the discovery of the radiation damage, ACIS has been protected during radiation belt passages. Radiation damage to the CCDs has continued at a much slower rate, due to soft protons scattered by the optics during observations, and strongly penetrating solar protons and cosmic rays which pass through the spacecraft shielding. The particle background on the detector consists of a quiescent portion that is anti-correlated with the solar cycle, and soft proton flares.

Suzaku is in a 96-minute, low-Earth orbit with an inclination of 32 degrees and gains some protection from cosmic rays by the Earth's geomagnetic field. Many orbits pass through the South Atlantic Anomaly (SAA), a region of enhanced particle flux, which requires the instruments to be shut off. The particle background on the detector is generally lower for XIS than for ACIS and varies throughout the orbit as a function of the geomagnetic cut-off rigidity, a measure of how well the Earth's geomagnetic field shields the spacecraft from charged particles.

2.3. Calibration Sources

Both ACIS and XIS have on-board radioactive ^{55}Fe sources used for instrument monitoring and calibration. The ACIS External Calibration Source (ECS), is mounted such that it is only viewable when ACIS is moved out of the focal plane. Observations of the ECS are done twice an orbit, just before and after perigee. The ECS provides roughly uniform illumination of the entire focal plane. Fluorescent Al and Ti targets provide lines at 1.5 keV (Al K) and 4.5 keV (Ti Kα), as well as those from the ^{55}Fe source itself at ~0.7 keV (Mn L), 5.9 keV (Mn Kα), and 6.4 keV (Mn Kβ)

The calibration sources on XIS illuminate the upper corners of each CCD (as shown in Figure 2) during all observations. The spectral lines are from the ^{55}Fe source itself at 5.9 keV (Mn Kα), and 6.4 keV (Mn Kβ). The orientation and approximate size of the regions illuminated by the calibration sources are shown in Figure 2.

3. Methodology

3.1. Data and Analysis

The data used here have not gone through the standard pipeline processing that is normally applied to data distributed to users. Standard processing is designed to remove some of the effects we are trying to study here, by applying corrections for charge transfer inefficiency and time-dependent gain changes. The actual performance seen by a typical user from standard pipeline processed data is much improved from that seen here. The data has been minimally processed, by removing the CCD bias level and by applying a standard grade filter to keep events with ASCA grades 0, 2, 3, 4, and 6 and discard all others. XIS1 and ACIS-S3 are used are representative BI CCDs and XIS3 and ACIS-I3 are representative FI CCDs.

As the XIS calibration sources only illuminate the upper corners of the CCDs, we filter the data to include only events within a rectangular region encompassing the calibration source events. The size of the region varies slightly between CCDs, but is roughly 225 pixels square. While the ACIS calibration sources fully illuminate the CCDs, the data were also filtered to roughly match the XIS regions.

3.2. A Proxy for Measuring CTI

A proper measurement of parallel CTI requires full illumination of the CCD with a source of known energy. ACIS is equipped with an External Calibration Source (ECS) comprising a ^{55}Fe source and aluminum and titanium targets that is capable of illuminating the entire CCD array with photons at a number of specific energies. The XIS instruments have fixed ^{55}Fe sources that illuminate the two corners farthest from the readout of each CCD with photons from Mn Kα (5.9 keV) and Mn Kβ (6.5 keV). Since the XIS calibration sources are incapable of illuminating the full chip, for proper comparison we must restrict our analysis to the upper corners of the ACIS chips as well. A change in CTI must change the accumulated charge loss and thus the pulseheight far from the framestore region. A change in pulseheight, however, does not necessarily have to be related to CTI; it could also be due to a changes in the gain completely unrelated to radiation damage.

ACIS has a known slow change in the gain as a function of time as measured very close to the framestore where CTI should be negligible. For all of the CCDs except I0 and I2 it is monotonically decreasing at a rate of ~ 1 ADU yr^{-1} at 5.9 keV.[1]

To determine the feasibility of using only the upper corners as a CTI metric, we compared the change in Mn Kα pulseheight to the measured CTI for two ACIS chips. The results are shown in Figure 3. Prior to correcting for the known gain change, the fractional pulseheight change is well-correlated to the CTI (left panels). After the correction, the correlation is even tighter (right panels). The correction coefficient was fit by eye, finding the

[1] See http://space.mit.edu/home/cgrant/gain for example plots of the gain change.

value the best reduced the ACIS-I3 scatter. The correction is always less than 0.5% of the total pulseheight.

- how relevant is this to XIS?

4. Discussion

4.1. CTI Time Evolution

The time evolution of CTI, as measured by the change in the line energy, is shown in Figures 4 and 5 for XIS and ACIS, respectively. The change in line energy is plotted as the fractional change since the first data point. Data from both front- and back-illuminated devices are included, as well as both with and without XIS charge injection.

Increasing CTI leads to decreasing measured line energy. All cases show an increase in CTI due to radiation damage. In some cases, the CTI increase from radiation damage is modified by sacrificial charge from the particle background, discussed further in Section 4.3. The rate of change of CTI varies substantially between the different cases.

4.1.1. Front- vs. Back-Illuminated Detectors

4.1.2. Chandra vs. Suzaku

4.2. Spectral Resolution Time Evolution

The time evolution of spectral resolution is shown in Figures 6 and 7 and XIS and ACIS, respectively. The spectral resolution is measured as the FWHM of the Mn Kα line.

4.2.1. Front- vs. Back-Illuminated Detectors

4.2.2. Chandra vs. Suzaku

4.3. CTI and Spectral Resolution: Dependence on Background

4.4. CTI and Spectral Resolution: Dependence on Temperature

At least some of the differences between the evolution of CTI on ACIS and XIS can possibly be due to operating at different focal plane temperatures. ACIS is much colder at -120°C than XIS at -90°C, so many of the common electron traps that cause CTI have been frozen out. In particular, the rate of change of CTI is much higher on XIS than ACIS. While this could be due to a higher level of damaging particle radiation, it could also be due to the higher CCD temperatures.

The ACIS team has performed a series of CTI measurements at different temperatures at two different times (Grant et al. 2006). By comparing the time evolution at -120°C and -90°C we can determine how large the CTI change on ACIS would be at either temperature.

5. Conclusions

Acknowledgements. The authors thank blah blah and blah blah for such and such. This work was supported by NASA grant so and so.

References

Bautz, M. W., LaMarr, B. J., Miller, E. D., et al. 2007, in Society of Photo-Optical Instrumentation Engineers (SPIE) Conference Series, Vol. 6686, Society of Photo-Optical Instrumentation Engineers (SPIE) Conference Series, ed. O. H. Siegmund

Garmire, G. P., Bautz, M. W., Ford, P. G., Nousek, J. A., & Ricker, Jr., G. R. 2003, in Society of Photo-Optical Instrumentation Engineers (SPIE) Conference Series, Vol. 4851, Society of Photo-Optical Instrumentation Engineers (SPIE) Conference Series, ed. J. E. Truemper & H. D. Tananbaum, 28–44

Gendreau, K., Bautz, M., & Ricker, G. 1993, Nuclear Instruments and Methods in Physics Research A, 335, 318

Grant, C. E., Bautz, M. W., Kissel, S. E., LaMarr, B., Prigozhin, G. Y. 2006 in Society of Photo-Optical Instrumentation Engineers (SPIE) Conference Series, Vol. 6276, Society of Photo-Optical Instrumentation Engineers (SPIE) Conference Series, ed. D. A. Dorn & A. D. Holland

Koyama, K., Tsunemi, H., Dotani, T., et al. 2007, PASJ, 59, 23

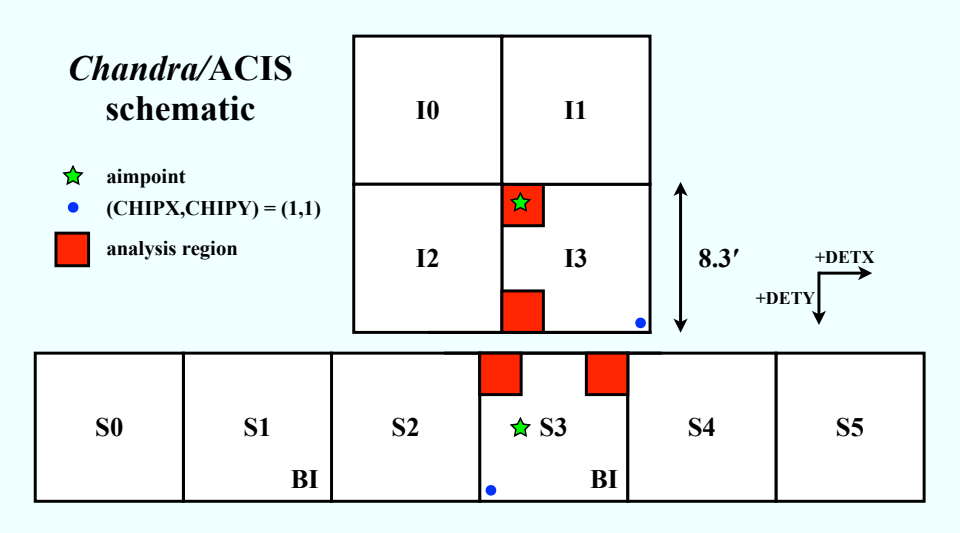

Fig. 1. Schematic drawing of the ACIS focal plane. The orange squares indicate the regions used for data analysis in this paper. The green stars show the standard aimpoints on ACIS-I3 and ACIS-S3.

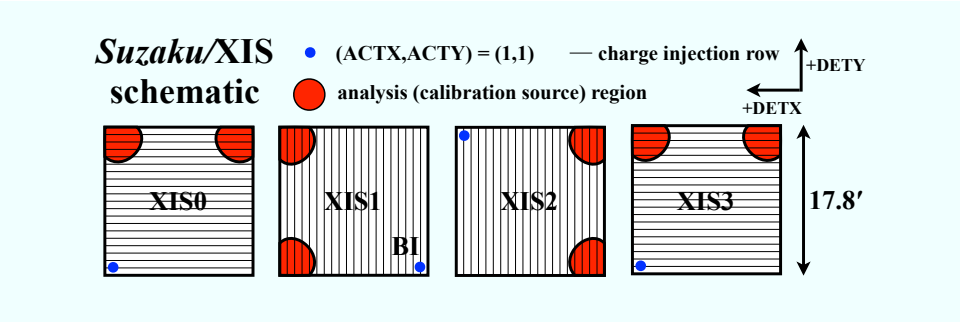

Fig. 2. Schematic drawing of the XIS focal plane. The orange circles show the regions illuminated by the ^{55}Fe sources. The light grey lines indicate the direction and spacing of the charge injection rows.

Table 1. Characteristics of MIT Lincoln Laboratory CCDs for ACIS and XIS

	ACIS	XIS
Model	CCID17	CCID41
Format	1026 rows × 1024 pixels/row (imaging area)	
Architecture	3-phase, frame-transfer, four parallel output nodes	
Illumination Geometry	8 FI & 2 BI	2 FI & 1 BI
Charge Injection Capable	no	yes
Pixel Size	24 × 24μm	
Readout Noise (RMS)	2–3 e$^-$ at 400 kpix s^{-1}	< 2.5 e$^-$ at 41 kpix s^{-1}
Depletion Depth	FI: 64–76 μm; BI: 30–40 μm	FI: 60–65 μm; BI: 40–45 μm
Operating Temperature	−120°C via radiative cooling	−90°C via Peltier cooler
Frame Exposure Time[a]	3.2 s	8.0 s
Pre-Launch CTI (10^{-5})	FI: < 0.3 BI: 1–3	FI: 0.3–0.5 BI: 0.55

[(a)] In normal operating mode.

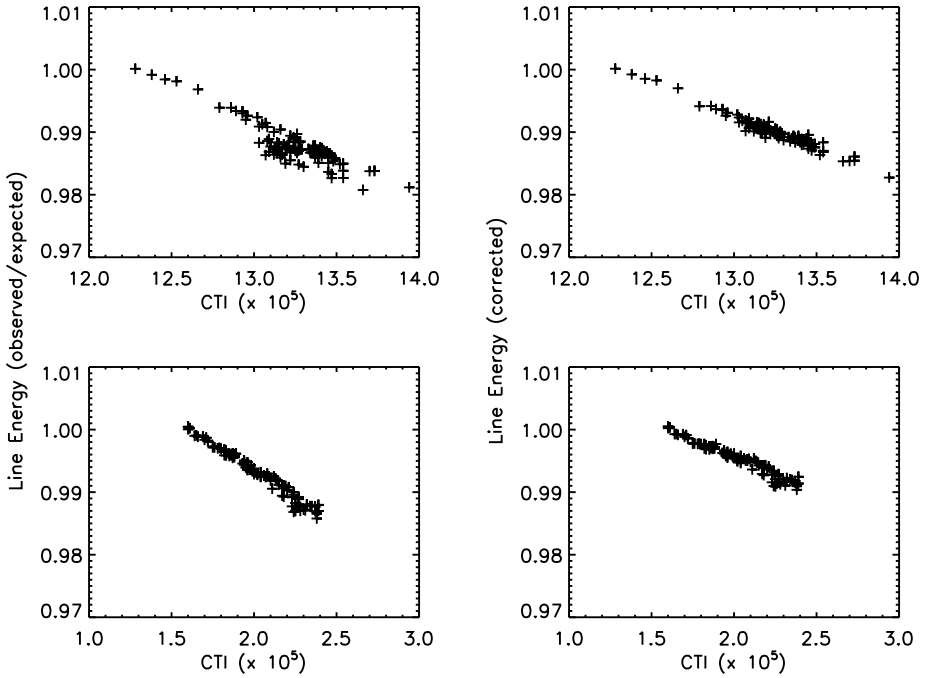

Fig. 3. CTI ($\times 10^5$) versus the fractional change in Mn Kα line energy for two ACIS devices, I3 (FI) and S3 (BI), as measured from the upper corners of each chip. The left panels show the measured data, while the right panels show data corrected for a slow gain decrease, discussed in the text. The CTI and pulseheight are well-correlated.

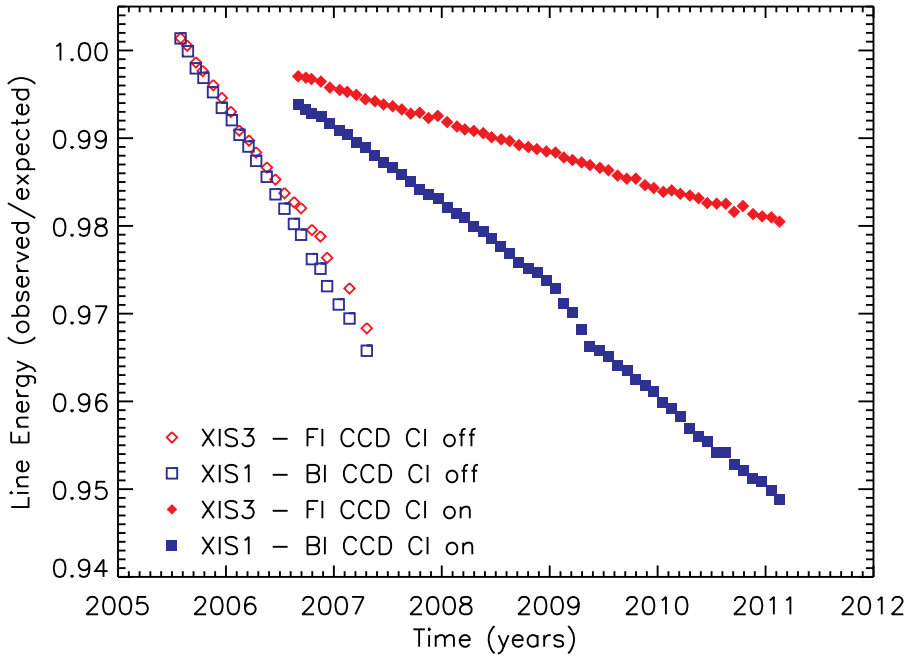

Fig. 4. Fractional change in the measured XIS central line energy over the course of the *Suzaku* mission, as measured at Mn Kα. Different symbols show FI and BI devices with charge injection (CI) on and off.

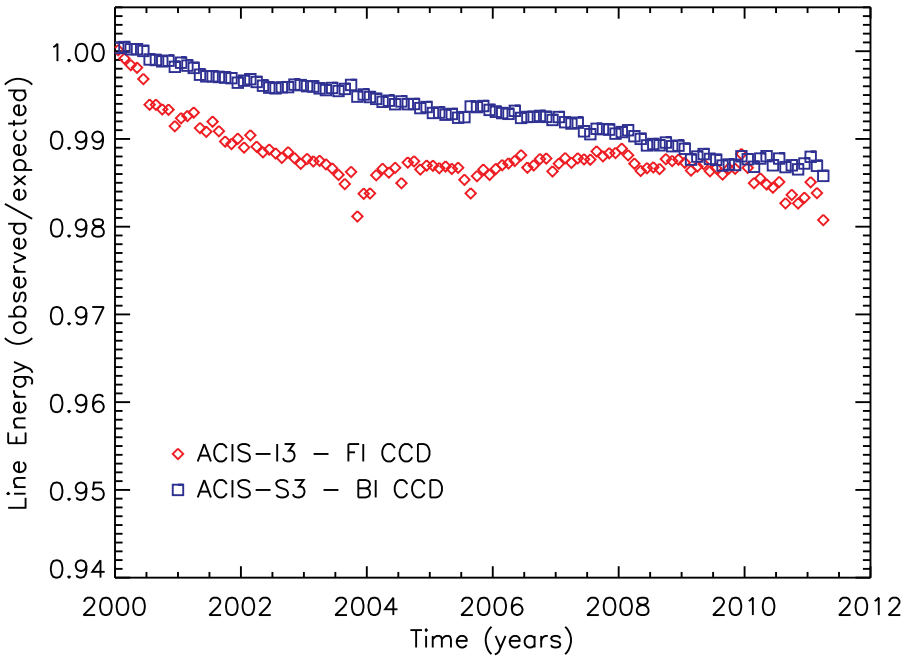

Fig. 5. Fractional change in ACIS line central energy over the course of the *Chandra* mission, as measured at Mn Kα. The effects of varying particle background and sacrifical charge are seen in the ACIS-I3 (FI) data.

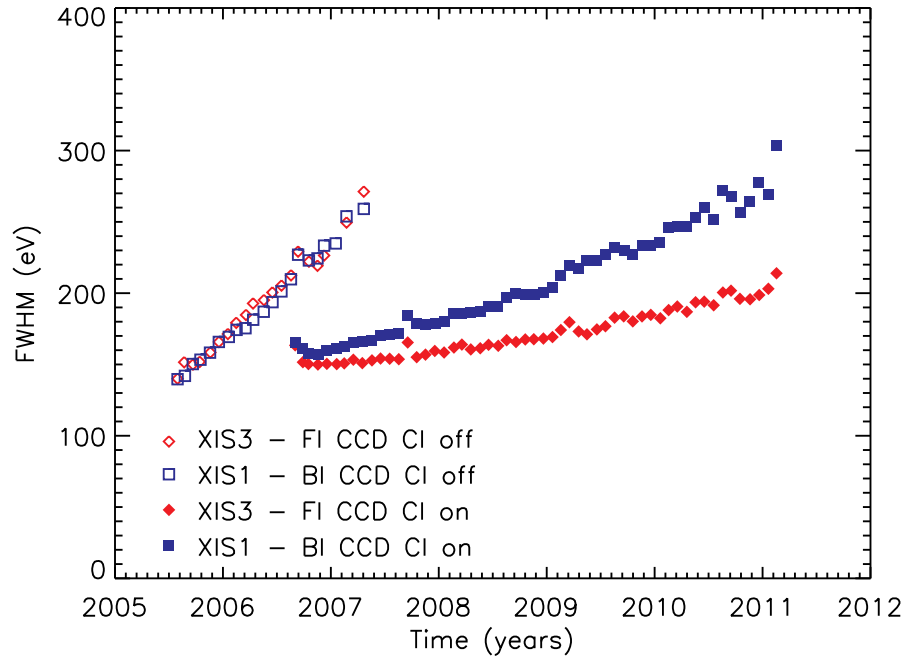

Fig. 6. Change in XIS line width (FWHM) with time over the course of the *Suzaku* mission, as measured at Mn Kα. Different symbols show FI and BI devices with charge injection (CI) on and off.

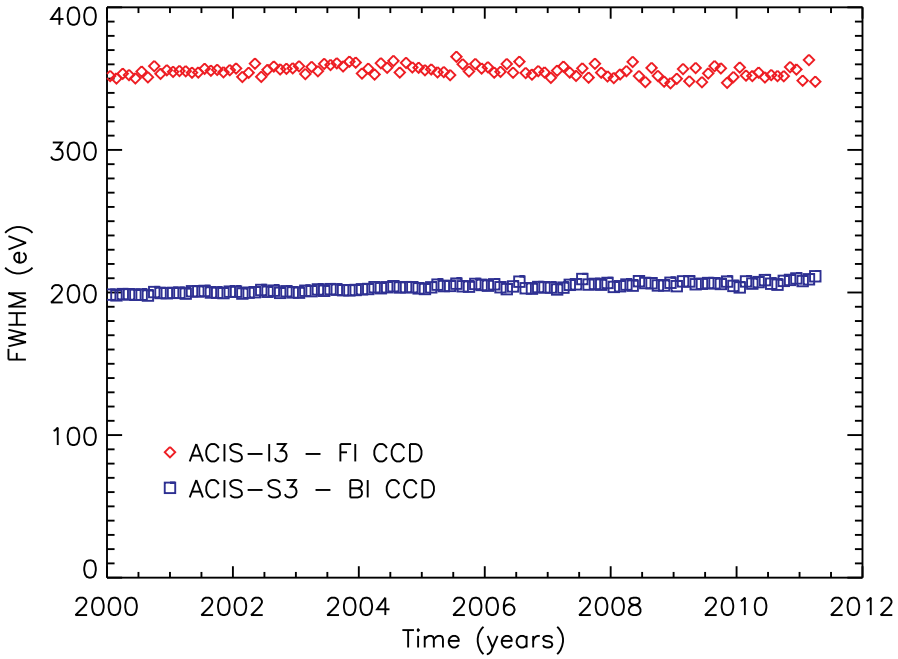

Fig. 7. Change in ACIS line width over the course of the *Chandra* mission, as measured at Mn Kα.

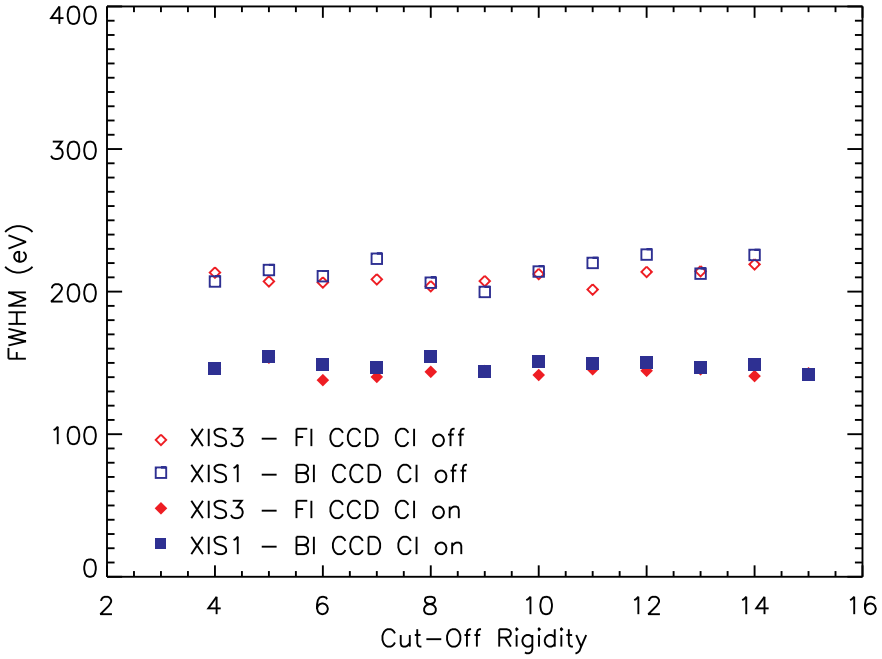

Fig. 8. XIS Mn Kα line width (FWHM) as a function of the geomagnetic cut-off rigidity (COR), averaging over October-November 2006. Symbols are the same as in Figure 6. Lower cut-off rigidity indicates a higher particle background, therefore the narrower line widths at low COR in the FI, CI off data (open points) are due to sacrificial charge. Use of CI overwhelms the effects of sacrificial, charge, so no dependence on COR is seen in those data (solid points).

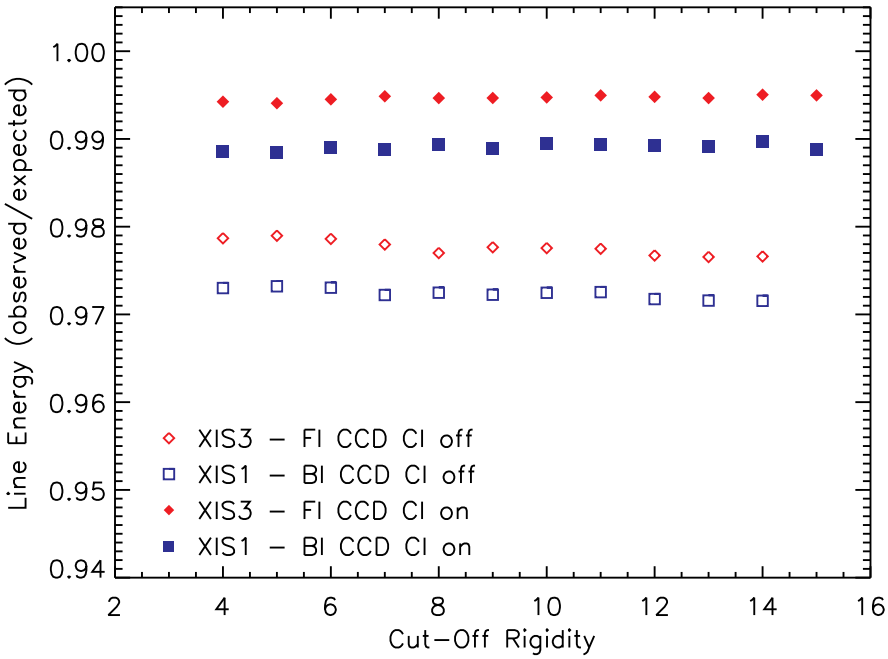

Fig. 9. Fractional change in the XIS line energy as a function of COR, averaging over October-November 2006. Symbols are the same as in Figure 4. A trend toward lower line energy (increased CTI) with higher COR (decreased background) is seen in the FI, CI off data. This results from lower amounts of sacrifical charge. As with the line width in Figure 8, use of CI overwhelms the effects of sacrificial charge (solid points).

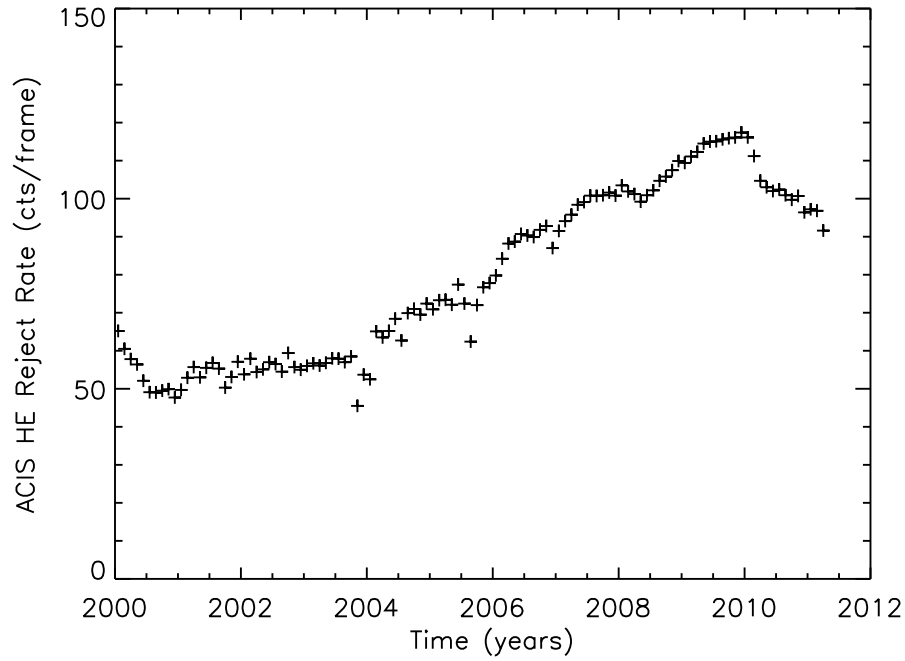

Fig. 10. Particle background over the course of the *Chandra* mission, measured as the rate of high energy events on ACIS-S3 (BI). The structure from the varying particle background can been seen in the ACIS line energy data.